frontiers | Frontiers in Mechanical Engineering

TYPE Original Research
PUBLISHED 27 February 2025
DOI 10.3389/fmech.2025.1547120

OPEN ACCESS

EDITED BY
Govind Vashishtha,
Wrocław University of Science and Technology, Poland

REVIEWED BY
Khandaker Noman,
Northwestern Polytechnical University, China
Hari Om,
IFTM University, India

*CORRESPONDENCE
Zongfang Zhang,
1455479587@qq.com

RECEIVED 17 December 2024
ACCEPTED 07 February 2025
PUBLISHED 27 February 2025

CITATION
Zhang Z and Zhang M (2025) Multi-parameter optimizations of elastic chain catenary based on response surface methodology for high-speed railway.
Front. Mech. Eng. 11:1547120.
doi: 10.3389/fmech.2025.1547120

Multi-parameter optimizations of elastic chain catenary based on response surface methodology for high-speed railway

Zongfang Zhang[1]* and Maoyou Zhang[2]

[1]School of Mechanical and Electrical Engineering, Xi'an Railway Vocational and Technical College, Xi'an, China, [2]China Construction Third Engineering Bureau Co., Ltd., Wuhan, China

As train operating speeds increase, the quality of pantograph-catenary current collection deteriorates, sometimes even resulting in contact loss. To ensure stable current collection during high-speed operation, it is crucial to optimize the design parameters of the catenary system. This study employs finite element analysis and constructs a pantograph-catenary coupling model using MSC. Marc software to simulate the coupled motion between the catenary and the pantograph. During the research process, the primary technical challenge was accurately evaluating the comprehensive effects of multi-parameter variations on pantograph-catenary current collection quality. First, we independently analyzed the effects of catenary tension and linear density variations on contact pressure to clarify the mechanisms of individual parameter influences. However, recognizing that multiple parameters might change simultaneously in actual operations, we introduced the Response Surface Methodology (RSM) to deeply explore the combined effects of two parameters on current collection quality. The innovation of this study lies not only in considering the effects of individual parameters but also in systematically analyzing the impact of multi-parameter interactions using RSM. Furthermore, from the perspective of the combined effects of catenary tension and contact wire linear density, we proposed an optimized catenary design scheme for the 500 km/h high-speed train operation scenario. Specifically, by increasing the contact wire tension, reducing the messenger wire tension, and lowering the linear density of the contact wire, we can significantly improve pantograph-catenary current collection quality, thereby providing robust support for the safe and stable operation of high-speed railways. In conclusion, this study addresses key technical challenges in multi-parameter optimization and proposes a practical optimization scheme with significant application value, offering important references for the design and optimization of high-speed railway catenary systems.

KEYWORDS

catenary, current collection quality, design parameters, response surface methodology, optimization

1 Introduction

In typical high-speed electrified railways, power is supplied to trains through the interaction between the pantograph and the catenary (Wu et al., 2022). The stability of this interaction, indicated by the contact pressure, directly reflects the quality of current collection (Pombo et al., 2009). As train speeds increase, disturbances from wheel-rail dynamics and aerodynamic forces exacerbate pantograph vibrations and catenary

oscillations (Luo et al., 2024). These effects lead to significant fluctuations in contact pressure, resulting in issues such as loss of contact and electrical arcing, which pose critical challenges to achieving higher operational speeds (Liu et al., 2023a).

Previously, extensive research has been conducted on current collection quality for high-speed pantograph-catenary systems (Liu et al., 2023b). Studies by Zhang et al. (2006) and Zhou and Zhang (2011), Zhou et al. (2011) have examined how different suspension types and structural parameters affect contact pressure. Jin Hee Lee and colleagues highlighted the importance of contact wire tension on current collection quality (Jin et al., 2015), while J. Pombo explored the impact of pantograph vibration characteristics and parameter adjustments on contact pressure (Pombo and Ambrósio, 2012). Mitsuo Aboshi analyzed how reflection coefficients affect current collection quality, and other studies investigated the influence of factors like pantograph speed and suspension stiffness on the dynamics of the pantograph-catenary system (Aboshi and Manabe, 2000).

Above mentioned previous studies have primarily focused on analyzing the impact of variations in individual parameters on the current collection quality of the pantograph-catenary system (Liu et al., 2023b; Zhang et al., 2006; Zhou and Zhang, 2011; Zhou et al., 2011; Jin et al., 2015; Pombo and Ambrósio, 2012; Aboshi and Manabe, 2000). However, during high-speed train operation, the intensified vibrations of the pantograph and oscillations of the contact wire make it challenging to meet current collection requirements by adjusting a single parameter alone.

Based on above discussions, this study considers the combined effects of multiple parameters and proposes an optimized catenary structure capable of ensuring stable current collection during high-speed operation. Building upon the analysis of individual parameter effects, this study employs the response surface methodology to evaluate the influence of pairwise parameter combinations on current collection quality. Response surface methodology has widely been used in optimization of the pantograph-catenary interactions in the high-speed railway systems (Wang et al., 2024; Su et al., 2023; Song et al., 2024; Liu et al., 2024). Furthermore, based on the simultaneous variation of multiple parameters, a specific design scheme for catenary parameters is proposed for trains operating at 500 km/h. This scheme offers meaningful guidance for the design of catenary parameters in high-speed railway systems.

2 Simulation of pantograph-catenary contact pressure

2.1 Pantograph-catenary coupling model

In this study, to improve the accuracy of contact pressure calculations in the pantograph-catenary system, an Euler-Bernoulli beam element was employed, taking into account factors such as droppers' stiffness and supporting devices. A finite element model of the catenary was established to simulate the motion of various nodes within the catenary system (Park et al., 2003).

In the model, the motion equation for each mass point of the contact wire is expressed as:

$$m_c\frac{\partial^2 u_c}{\partial t^2}+\frac{\partial^2}{\partial x^2}\left(EI_c\frac{\partial^2 u_c}{\partial x^2}\right)-\frac{\partial}{\partial x}\left(T_c\frac{\partial u_m}{\partial x}\right)+k_d\left(u_m-u_c\right)\delta\left(x-x_n\right)=F\delta\left(x-vt\right) \tag{1}$$

In the Equation 1, M_c represents the unit mass of the contact wire, EI_c denotes the bending stiffness of the contact wire, and T_c indicates the tension in the contact wire. The Dirac delta function δ accounts for the impact forces, while F represents the contact pressure between the pantograph and the contact wire. The displacement of the contact wire is denoted as u_c, and u_m represents the displacement of the messenger wire. Furthermore, x_n is the distance between the dropper point and the motion point, x is the position of the motion point, t represents the motion time, and v is the train's operating speed.

The motion equation for the load-bearing cable is:

$$m_m\frac{\partial^2 u_m}{\partial t^2}+\frac{\partial^2}{\partial x^2}\left(EI_m\frac{\partial^2 u_m}{\partial x^2}\right)-\frac{\partial}{\partial x}\left(T_m\frac{\partial u_m}{\partial x}\right)+k_d\left(u_m-u_c\right)\delta\left(x-x_n\right)+k_s u_m\left(x-x_s\right)=0 \tag{2}$$

In the Equation 2, m_m represents the unit mass of the load-bearing cable; EI_m denotes the bending rigidity of the cable; T_m is the tension in the load-bearing cable; k_d indicates the stiffness of the suspension wire; k_s refers to the equivalent stiffness of the supporting device; and x_s is the distance between the support point and the motion point.

A three-mass model, which reflects the high-frequency vibrations of the pantograph, is adopted (Massat et al., 2006; Bruni et al., 2018; Cho et al., 2010). The equation of motion is given by Equation 3:

$$\begin{cases} m_1\ddot{y}_1+c_1\dot{y}_1+k_1y_1-c_1\dot{y}_2-k_1y_2=-F(t) \\ m_2\ddot{y}_2+(c_1+c_2)\dot{y}_2+(k_1+k_2)y_2-c_2\dot{y}_3 \\ -k_2y_3-c_1\dot{y}_1-k_1y_1=0 \\ m_3\ddot{y}_3+(c_2+c_3)\dot{y}_3+(k_2+k_3)y_3- \\ c_2\dot{y}_2-k_2y_2=F_0 \end{cases} \tag{3}$$

In the equation, m_1 represents the mass of the pantograph head; m_2 is the mass of the upper frame; m_3 denotes the mass of the pantograph lower frame; k_i indicates the equivalent stiffness;c_i refers to the equivalent damping; $F(t)$ is the contact pressure between the pantograph and the overhead contact wire; and F_0 is the static lifting force provided to the pantograph by the push rod.

In the parameter design of the model, the contact network adopts the elastic chain suspension structure of the Beijing-Tianjin Intercity High-Speed Railway, and the pantograph employs the Faiveley single-slide pantograph structure. The specific design parameters of the pantograph-wire system are shown in Figure 1. Based on the contact network-pantograph structure and parameters shown in Figure 2, a simulation model of the full-anchor segment elastic chain suspension contact network and single-slide pantograph is established using MSC. marc simulation software, as depicted in Figure 2.

In this study, the pantograph-wire model is validated according to the European railway standard EN50318 (EN50318, 2002). Based on the pantograph-wire parameters provided in the EN50318 standard, an Euler-Bernoulli beam contact network

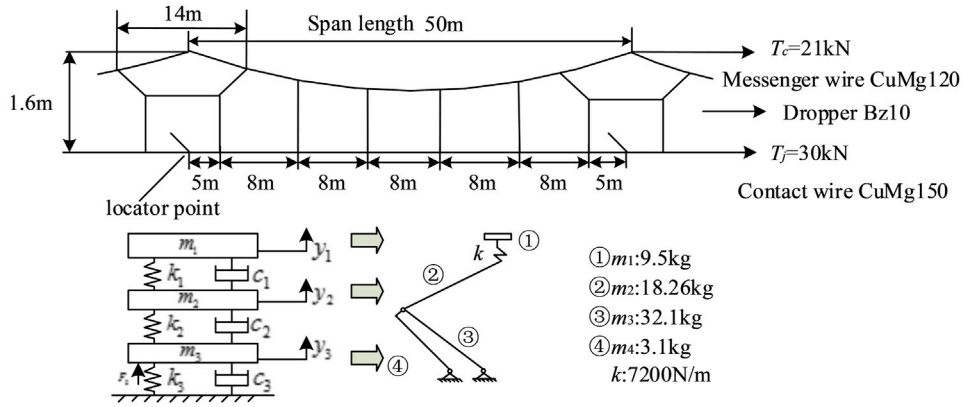

FIGURE 1
Schematic diagram of the elastic chain contact network and pantograph coupling model structure.

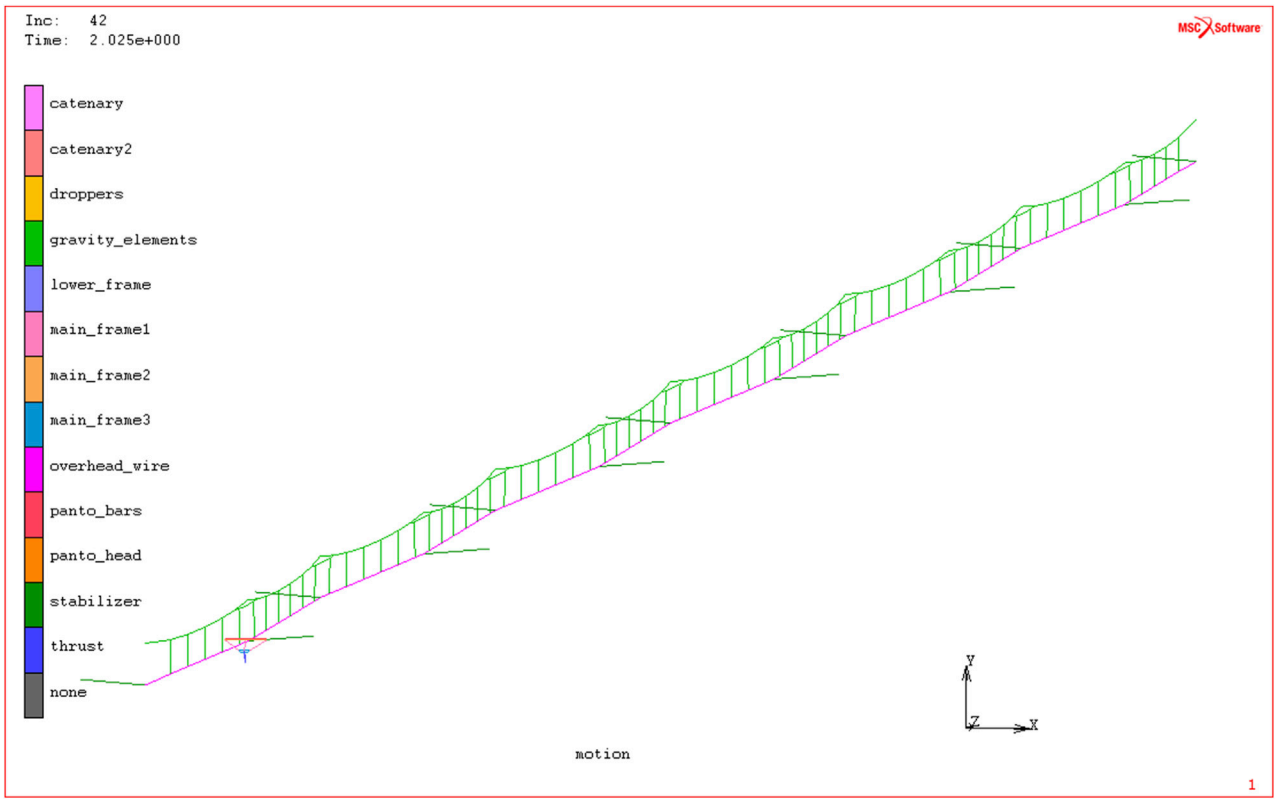

FIGURE 2
Simulation model of the elastic chain contact network and pantograph system.

model and a three-mass pantograph model are established in MSC. Marc. The contact pressure at operating speeds of 250 km/h and 300 km/h is calculated and compared with the specified range in the EN50318 standard, as shown in Table 1.

As shown in Table 1, under the operating speeds of 250 km/h and 300 km/h, the simulation results obtained from the modeling in MSC. Marc fall within the specified range of the EN50318 standard. This confirms the feasibility of establishing the pantograph-wire finite element model in MSC.marc.

2.2 Relationship between catenary design parameters and contact pressure

Under a constant pantograph speed, contact pressure across various points within a span is influenced by the catenary's elasticity and line mass. This can be described with the following dynamic equation (Li et al., 2022):

$$F = (1/\eta)u + C\dot{u} + M\ddot{u} \quad (4)$$

TABLE 1 Statistical data of pantograph-wire simulation results and the specified range in EN50318 standard.

Indicator name	Specified range in EN50318 standard		Simulation model calculation results	
Speed level	250 km/h	300 km/h	250 km/h	300 km/h
Average value/N	110 ~ 120	110 ~ 120	110.98	110.00
Standard deviation/N	26 ~ 31	32 ~ 40	29.31	33.75
Statistical maximum value (N)	190 ~ 210	210 ~ 230	198.92	211.23
Statistical minimum value (N)	20 ~ 40	−5 ~ 20	23.05	8.76
Actual maximum value (N)	175 ~ 210	190 ~ 225	207.98	223.03
Actual minimum value (N)	50 ~ 75	30 ~ 55	59.64	45.62
Maximum lift at locating point/mm	48 ~ 55	55 ~ 65	54.91	63.05
Offline rate/%	0	0	0	0

In the equation, F represents the contact pressure; η is the elasticity of the overhead contact line particle; C is the damping of the overhead contact line particle; M is the mass of the overhead contact line particle. Under the condition of neglecting the mass of the suspension wires and locating points, M is composed of the mass of the contact line and the carrying cable. u represents the vertical displacement of the contact suspension particle; $\dot{u}$ is the vertical velocity of the overhead contact line particle; and $\ddot{u}$ is the vertical acceleration of the overhead contact line particle.

The elasticity at each position point within a span of the overhead contact line can be expressed as follows:

$$\eta = x(l-x)\Big/\Big(l\big(T_c + T_j\big)\Big) \tag{5}$$

In the equation, x represents the position of a point within the span; l is the span length; T_c and T_j represent the tension in the carrying cable and the contact line, respectively.

Substituting Equation 5 into Equation 4 yields:

$$F = l\big(T_c + T_j\big)\cdot u\Big/\left(x(l-x)\right) + C\dot{u} + M\ddot{u} \tag{6}$$

From the above Equation 6, it can be seen that, under the condition of not changing the structural parameters of the overhead contact line — that is, without altering the span length, the spacing of the suspension wires, the structural height, and other parameters — the contact pressure at each point within the span is primarily related to the tension in the contact line and the design parameters of the line's mass.

3 Effects of catenary parameter changes on contact pressure

The average value and standard deviation of the contact pressure are important indicators for measuring the quality of current collection between the pantograph and the overhead contact line. The following analysis will use the average contact pressure and standard deviation as evaluation metrics to examine the impact of individual variations in contact line design parameters on contact pressure, as well as the effects of combinations of two variables changing simultaneously on contact pressure.

3.1 Influence of single parameter variations on contact pressure

3.1.1 Tension in the overhead contact line

Based on the simulation model in Section 2.1, the effects of changes in the contact line tension and the supporting cable tension on the contact pressure are analyzed separately. When analyzing the effect of contact line tension, other parameters are kept constant, with the train running at a speed of 300 km/h. The contact pressure curves are calculated for contact line tensions of 21 kN, 24 kN, 27 kN, 30 kN, and 30 kN. Similarly, the contact pressure curves are calculated for supporting cable tensions of 15 kN, 18 kN, 21 kN, 24 kN, and 27 kN. Figures 3A, B show the contact pressure curves under varying contact line and supporting cable tensions.

From Figures 3A,B, it can be seen that the contact pressure curve exhibits periodic variation with the span as a cycle. Within one cycle, there is a peak in contact pressure near the positioning points, while the pressure is relatively low in the middle of the span. This is because the stiffness of the catenary near the positioning points is high, which limits the lifting of the pantograph, making it difficult to raise the contact line. On the other hand, the stiffness of the catenary in the middle of the span is lower, allowing the contact line to be lifted more easily, hence the observed phenomenon. As the tension in the contact line and supporting cable increases, the contact pressure curve generally shifts upwards. This is due to the fact that increasing the line tension enhances the overall stiffness of the catenary, leading to an increase in the average contact pressure. From Figure 3A, it can be observed that increasing the contact line tension tends to reduce the peak contact pressure, while in Figure 3B, increasing the supporting cable tension tends to increase the peak contact pressure. This is because increasing the contact line tension reduces the unevenness in the stiffness of the catenary, whereas increasing the supporting cable tension increases the stiffness unevenness of the catenary. Therefore, in Figures 3A, B, the variation in peak contact pressure shows opposite trends with respect to the changes in the tensions of the contact line and the supporting cable.

3.1.2 Catenary wire line density

Based on the simulation model presented in Section 2.1, the effects of variations in the contact wire line density and supporting

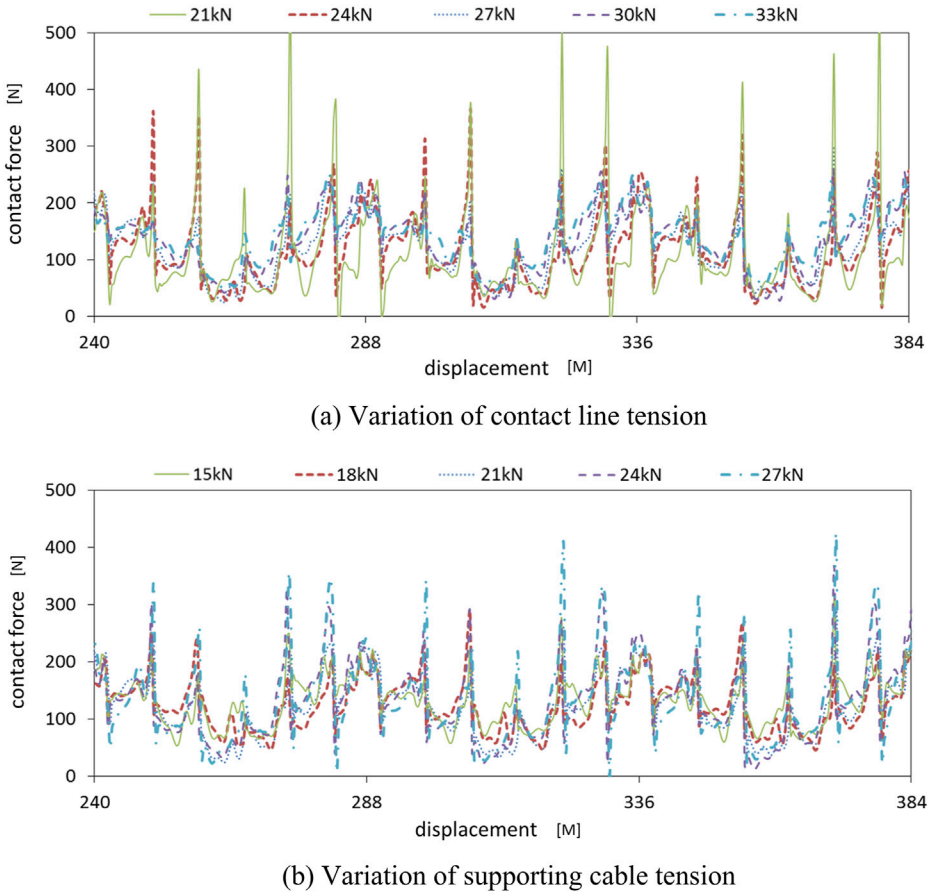

FIGURE 3
Contact pressure variation curve with changes in tension of the contact line. **(A)** Variation of contact line tension. **(B)** Variation of supporting cable tension.

cable line density on the contact pressure are analyzed. When discussing the effect of wire line density, all other parameters are kept constant, with the train operating speed set at 300 km/h. The contact pressure curves are calculated for contact wire and supporting cable line densities of 0.78 kg/m, 0.93 kg/m, 1.08 kg/m, 1.23 kg/m, and 1.38 kg/m, as shown in Figure 4.

From Figures 4A, B, it can be observed that as the wire line density increases, the amplitude of the contact pressure curve increases. The contact pressure value in the middle span decreases, while the peak value near the contact point increases. This is due to the increase in the wire line density, which enhances the inertia of the catenary system, making it harder for the operating state of the catenary to change. When the pantograph and contact wire move in contact with each other, the larger mass of the catenary leads to an opposite or relative motion between the pantograph and the contact wire. As a result, increasing the wire line density causes the amplitude variation of the contact pressure curve to become larger.

In summary, within a certain range, modifying a single parameter of the catenary system—such as increasing the contact wire tension, reducing the supporting cable tension, or decreasing the line density of the contact wire or supporting cable-can improve the quality of pantograph-catenary current collection.

3.2 Dual parameter variation analysis using response surface methodology

To further discuss the influence of the combination of contact wire tension, catenary tension, contact wire linear density, and catenary linear density on contact pressure, this paper introduces the response surface method to conduct experiments, modeling, and data analysis between catenary design parameters and contact pressure. By establishing the functional relationship between independent variables and dependent variables, the contour maps of the combination of various factors are obtained, and the optimal value of the response and combination parameters are predicted.

In this paper, the most common test method in response surface analysis, namely, the central composite experiment (Lundstedt et al., 1998; Bartz-Beielstein et al., 2010), is used. The test points of the two-level central composite design are shown in Figure 5.

To analyze the train operating speed at 300 km/h, this design takes four catenary design parameters as independent variables and the statistical values of contact pressure as the dependent variable. A response surface methodology analysis was conducted to study the relationship between them. As discussed in the previous section, there is a significant functional relationship between the contact wire tension, messenger wire tension, contact wire linear density, and messenger wire linear density and the statistical indicators of contact

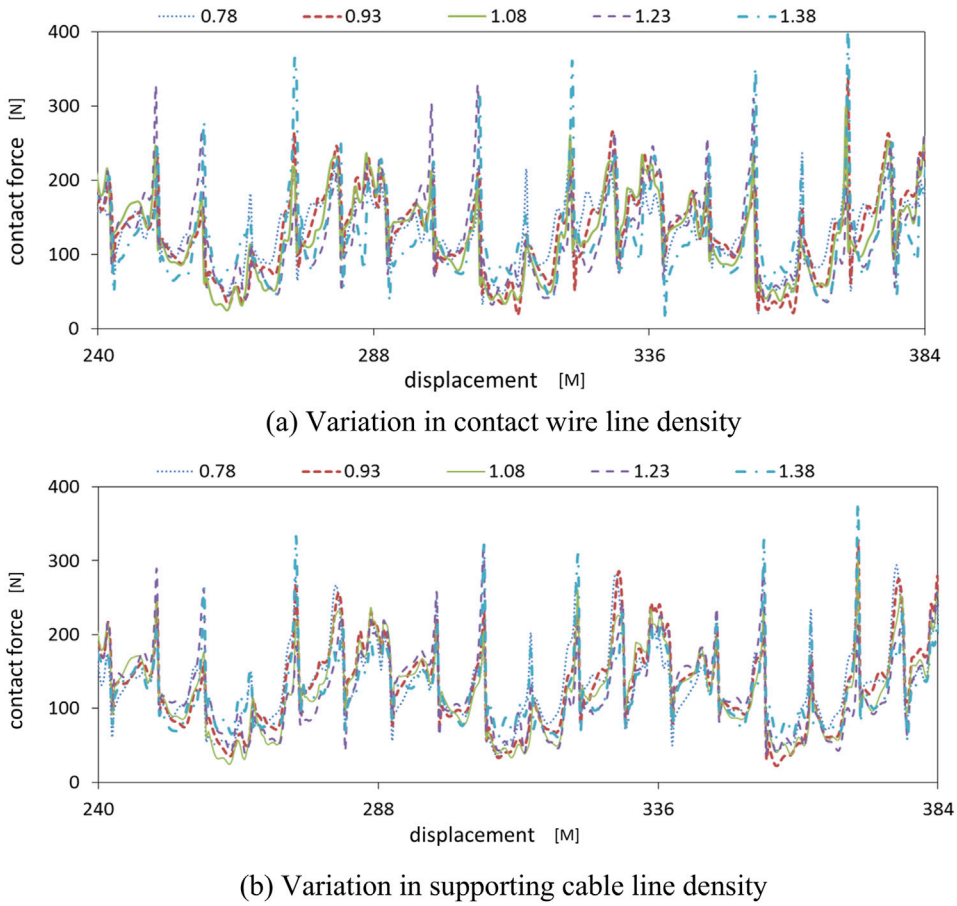

FIGURE 4
Variation of contact pressure curve with changes in wire line density. **(A)** Variation in Contact Wire Line Density. **(B)** Variation in Supporting Cable Line Density.

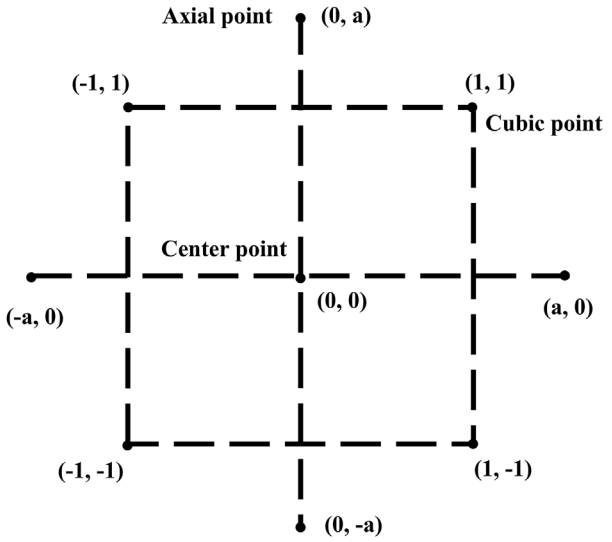

FIGURE 5
Test points of central composite design.

pressure. However, this relationship is not strictly linear. Therefore, the regression equation is set as a second-order interaction nonlinear model (2FI model), which is expressed as Equation 7:

$$F_x = F_0 + a_1T_c + a_2T_j + a_3m_c + a_4m_j + b_1T_cT_j + b_2T_cm_c + b_3T_cm_j + c_1T_jm_c + c_2T_jm_j + d_1m_cm_j \quad (7)$$

Here, Fx represents the contact pressure indicators; Tc represents the messenger wire tension, Tj represents the contact wire tension, mc represents the messenger wire linear density, and mj represents the contact wire linear density. According to the principle of central composite experiment design, a total of 30 experiments is conducted in this paper.

The basic parameters of the catenary are T_{j0} = 27 kN, T_{c0} = 21 kN, M_{j0} = 1.08 kg/m, and M_{c0} = 1.08 kg/m. Design-Expert 8.0 is used to perform response surface analysis on the experimental data, and contour maps of the maximum contact pressure and the standard deviation of contact pressure are obtained respectively. As shown in Figures 6, 7, the analysis results are shown in Tables 2, 3 respectively.

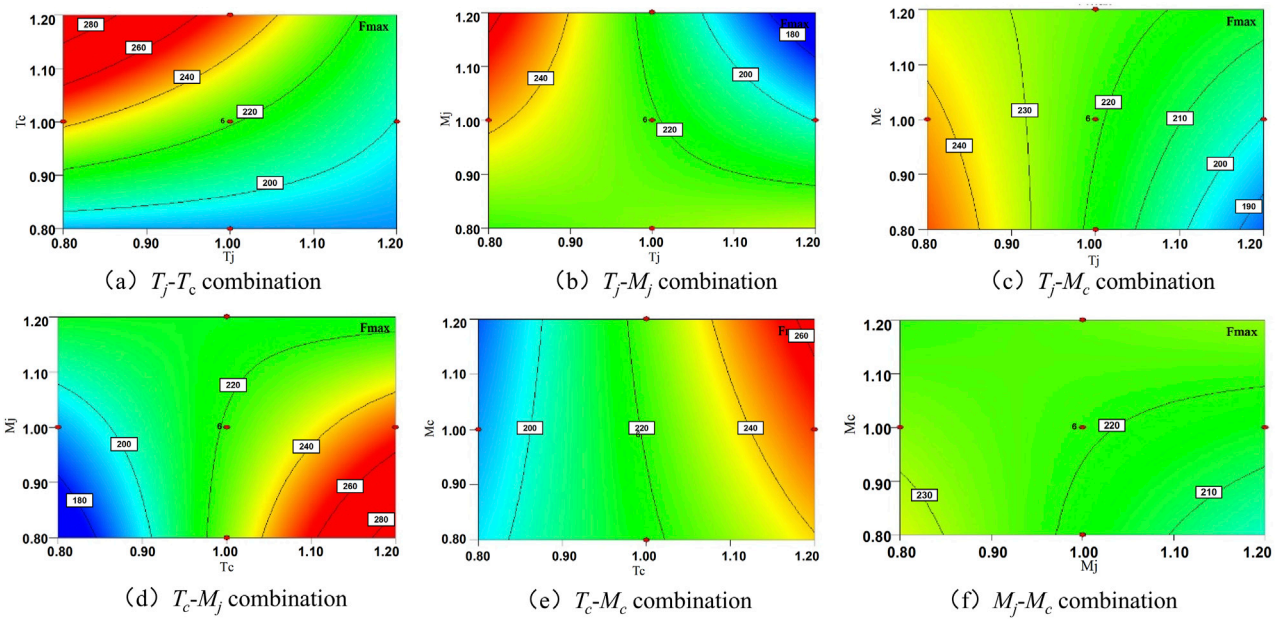

FIGURE 6
Contour map of the maximum contact pressure at 300 km/h. **(A)** T_j-T_c combination **(B)** T_j-*Mj* combination **(C)** T_j-*Mc* combination **(D)** T_c-*Mj* combination **(E)** T_c-*Mc* combination **(F)** *Mj*-*Mc* combination.

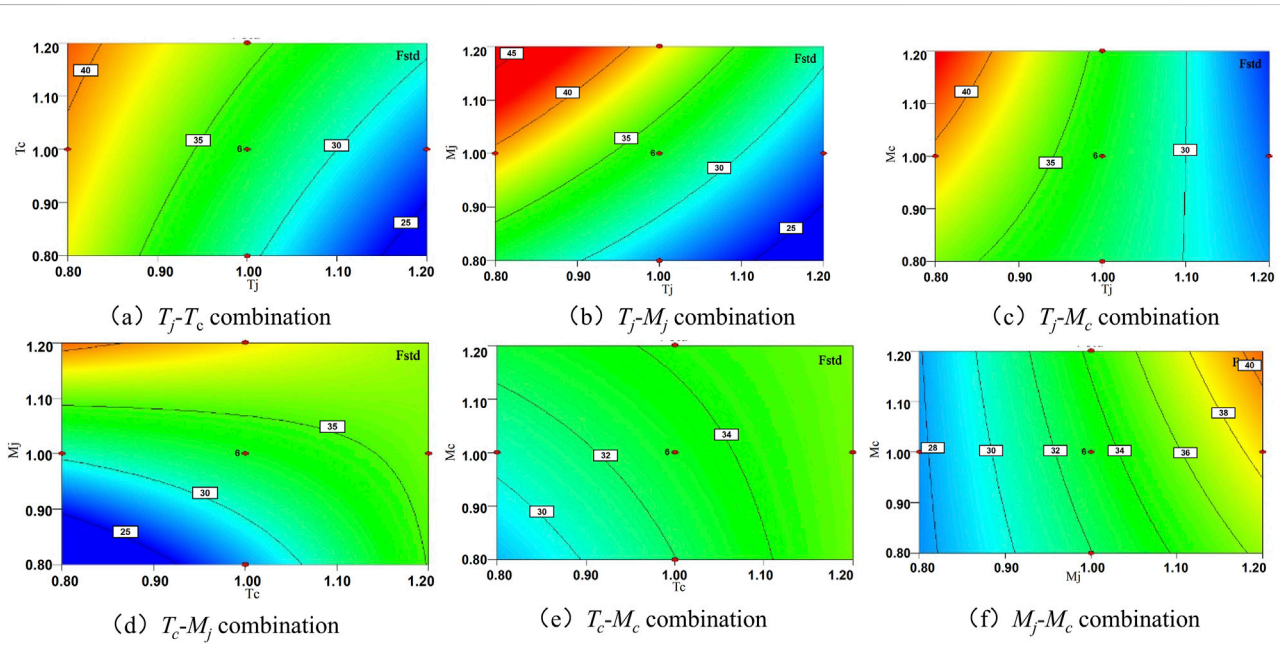

FIGURE 7
Contour map of the standard deviation of contact pressure at 300 km/h. **(A)** T_j-T_c combination **(B)** T_j-*Mj* combination **(C)** T_j-*Mc* combination **(D)** T_c-*Mj* combination **(E)** T_c-*Mc* combination **(F)** *Mj*-*Mc* combination.

According to Figure 6; Table 2, at a speed level of 300 km/h, when the design parameters change simultaneously, increasing the contact wire tension, reducing the catenary tension, and reducing the linear density of the contact wire can lead to a consistent decreasing trend in the standard deviation of contact pressure. However, the influence of the linear density of the catenary on the standard deviation of contact pressure is inconsistent when combined with different parameter combinations, and the combined effect with other parameters needs to be considered. According to the overall changing trend, the parameter combination that minimizes the standard deviation of contact pressure within the test area is in the neighborhood of (T_j = 1.2T_{j0}, T_c = 0.8T_{c0}, M_j =

TABLE 2 Trend of maximum value with parameters.

Parameter combination	Direction of Fmax reduction	Direction of Fmax increase
(T_j, T_c)	(1.2, 0.8)	(0.8, 1.2)
(T_j, M_j)	(1.2, 0.8)	(0.8, 1.2)
(T_j, M_c)	(1.2, 1.2)	(0.8, 0.8)
(T_c, M_j)	(0.8, 0.8)	(1.2, 1.2)
(T_c, M_c)	(0.8, ---)	(1.2, ----)
(M_j, M_c)	(1.2, 1.2)	(0.8, 0.8)

TABLE 3 Trend of standard deviation with parameters.

Parameter combination	Direction of Fmax reduction	Direction of Fmax increase
(T_j, T_c)	(1.2, 0.8)	(0.8, 1.2)
(T_j, Mj)	(1.2, 0.8)	(0.8, 1.2)
(T_j, Mc)	(1.2, 0.8)	(0.8, 1.2)
(T_c, Mj)	(0.8, 0.8)	(1.2, 1.2)
(T_c, Mc)	(0.8, 0.8)	(1.2, 1.2)
(Mj, Mc)	(0.8, 0.8)	(1.2, 1.2)

$0.8M_{j0}$, $M_c = 1.2M_{c0}$). At 300 km/h, to minimize the maximum contact pressure, the catenary parameters need to be optimized in this direction.

According to Figure 7; Table 3, at a speed level of 300 km/h, when the design parameters change simultaneously, increasing the contact wire tension, reducing the catenary tension, and reducing the linear density of the contact wire can lead to a consistent decreasing trend in the standard deviation of contact pressure. However, the influence of the linear density of the catenary on the standard deviation of contact pressure is inconsistent when combined with different parameter combinations, and the combined effect with other parameters needs to be considered. According to the overall changing trend, the parameter combination that minimizes the standard deviation of contact pressure within the test area is in the neighborhood of ($T_j = 1.2T_{j0}$, $T_c = 0.8T_{c0}$, $M_j = 0.8M_{j0}$, $M_c = 1.2M_{c0}$). This indicates that under the condition of 300 km/h, to minimize the standard deviation of contact pressure, the catenary parameters need to be optimized in this direction.

From the above analysis, when two parameters are combined with each other, the contact wire tension and catenary tension are important factors affecting the contact pressure. When the linear density of the catenary and the tension of the wires are combined respectively, the main variable affecting the contact pressure is the wire tension, while the influence of the linear density of the catenary is very small.

Considering the influence of the change of catenary parameters on the standard deviation and average value of contact pressure comprehensively, when the train running speed is 300 km/h, increasing the contact wire tension, reducing the catenary tension, and reducing the linear density of the contact wire can improve the current collection quality of the pantograph-catenary system.

4 Catenary parameter optimization at 500 km/h

When the train running speed is 500 km/h, there are more off-line points between the pantograph and catenary. Therefore, the influence of the pairwise combination of catenary parameters on the maximum contact pressure, the standard deviation of contact pressure, and the off-line rate will be discussed below.

The contour map of the maximum contact pressure at a running speed of 500 km/h is shown in Figure 8.

According to Figure 8; Table 4, it can be known that at a speed level of 500 km/h, when the design parameters change simultaneously, increasing the contact wire tension, increasing the messenger wire tension, and reducing the contact wire linear density can make the standard deviation of contact pressure show a consistent decreasing trend. However, the influence of the messenger wire linear density on the standard deviation of contact pressure is inconsistent when combined with different parameter combinations, and the combined effect with other parameters needs to be considered. According to the overall change trend, the parameter combination that minimizes the standard deviation of contact pressure within the test area is in the neighborhood of ($T_j = 1.2T_{j0}$, $T_c = 1.2T_{c0}$, $M_j = 0.8M_{j0}$, $M_c = 0.8M_{c0}$). At 500 km/h, to minimize the standard deviation of contact pressure, the catenary parameters need to be optimized in this direction.

The contour map of the standard deviation rate of contact pressure under the condition of an operating speed of 500 km/h is shown in Figure 9.

According to Figure 9; Table 5, at a speed level of 500 km/h, when the design parameters change simultaneously, increasing the contact wire tension, reducing the catenary wire tension, and

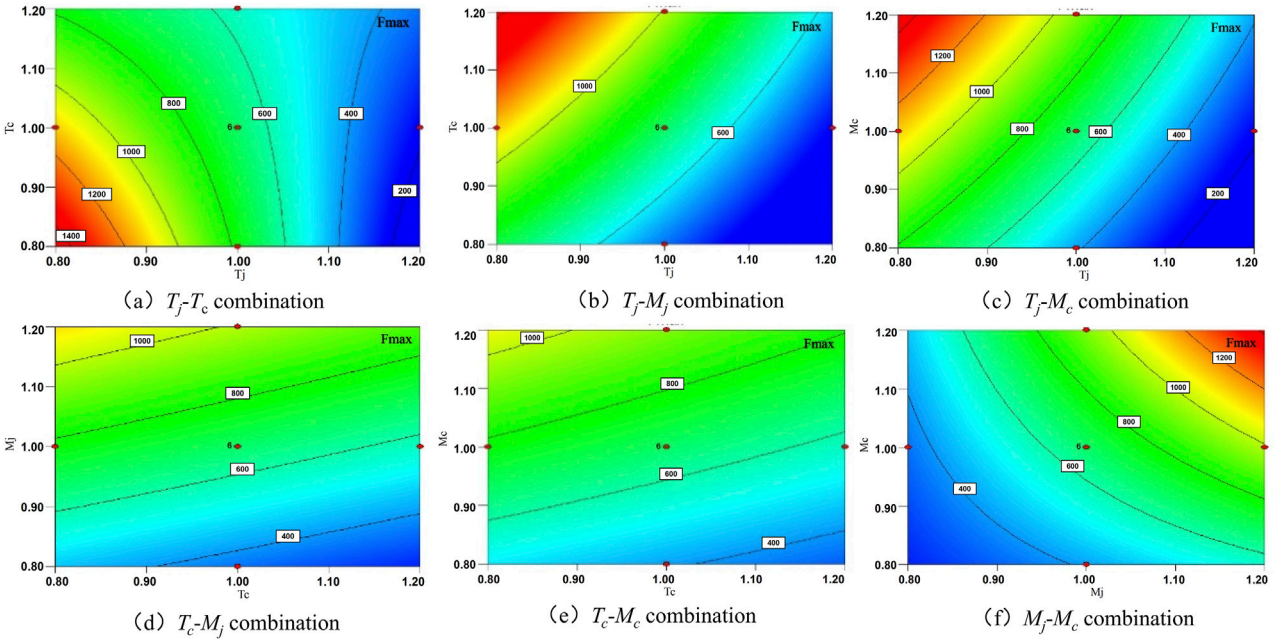

FIGURE 8
Contour map of the maximum contact pressure at 500 km/h. **(A)** T_j-T_c combination **(B)** T_j-Mj combination **(C)** T_j-Mc combination **(D)** T_c-Mj combination **(E)** T_c-Mc combination **(F)** Mj-Mc combination.

TABLE 4 The variation trend of the maximum value with parameters.

Parameter combination	Direction of Fmax reduction	Direction of Fmax increase
(T_j, T_c)	(1.2, 1.2)	(0.8, 0.8)
(T_j, Mj)	(1.2, 0.8)	(0.8, 1.2)
(T_j, Mc)	(1.2, 0.8)	(0.8, 1.2)
(T_c, Mj)	(1.2, 0.8)	(0.8, 1.2)
(T_c, Mc)	(1.2, 0.8)	(0.8, 1.2)
(Mj, Mc)	(0.8, 0.8)	(1.2, 1.2)

reducing the contact wire linear density can make the standard deviation of contact pressure show a consistent decreasing trend. However, when the catenary wire linear density is combined with different parameter combinations, the influence on the standard deviation of contact pressure is inconsistent, and the combined effect with other parameters needs to be considered. According to the overall variation trend, the parameter combination that minimizes the standard deviation of contact pressure within the test area is in the neighborhood of (T_j = 1.2T_{j0}, T_c = 1.2T_{c0}, M_j = 0.8M_{j0}, M_c = 0.8M_{c0}). This indicates that under the condition of 500 km/h, to minimize the standard deviation of contact pressure, the catenary parameters need to be optimized in this direction. The off-line contour map of contact pressure under the condition of an operating speed of 500 km/h is shown in Figure 10.

As can be seen from Figure 10 and Table 6, at a level of 500 km/h, the influence trends of various parameters on the off-line rate are not consistent. Increasing the tension of the contact wire, reducing the tension of the catenary wire, and reducing the linear density of the contact wire all reduce the off-line rate under any combination. The change of the linear density of the catenary wire is not consistent according to different combinations. In comprehensive consideration, the parameter combination that can reduce the off-line rate is within the neighborhood of (T_c = 0.8T_{c0}, T_j = 1.2T_{j0}, M_c = 1.2M_{c0}, M_j = 0.8M_{j0}).

According to the analysis of the response surface contour map of the maximum contact pressure, standard deviation, and off-line rate at a speed level of 500 km/h, when changing the linear density of the catenary wire under different parameter combinations, the influence on the standard deviation of contact pressure is consistent, but the influence on the off-line rate is inconsistent. However, considering the overall change of contact pressure, the optimization direction is (T_c = 0.8T_{c0}, T_j = 1.2T_{j0}, M_c = 1.2M_{c0}, M_j = 0.8M_{j0}), that is, increasing the tension of the contact wire, reducing the tension of the catenary wire, reducing the linear density of the contact wire, and increasing the linear density of the catenary wire.

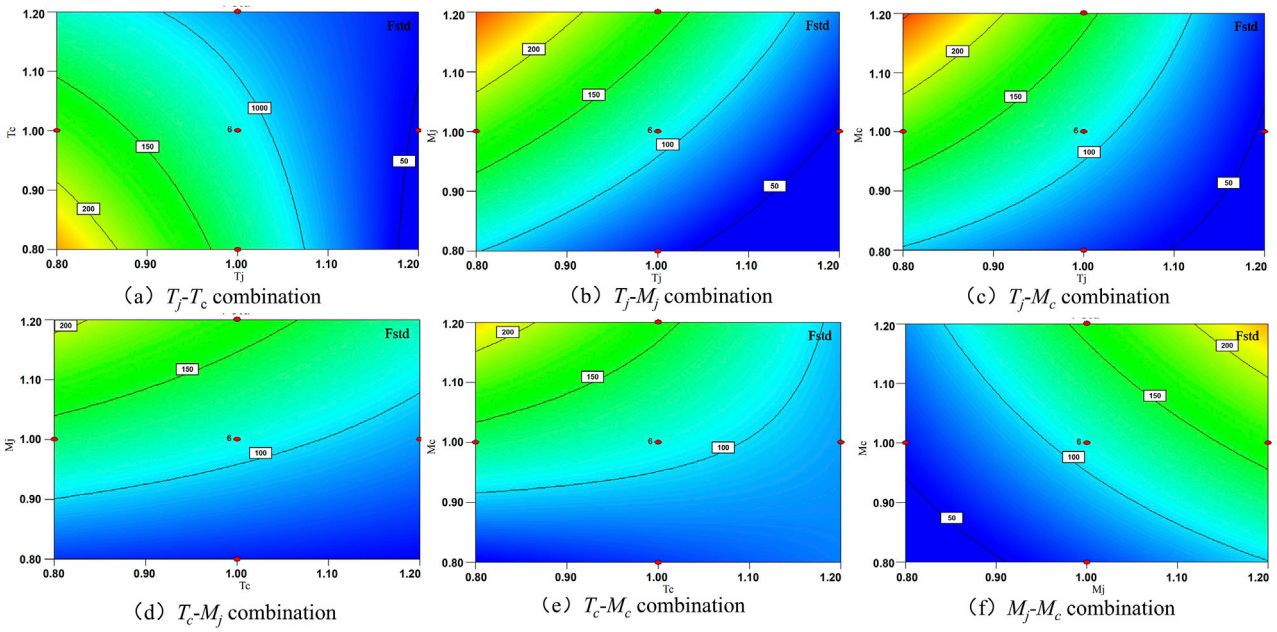

FIGURE 9
Contour map of standard deviation at 500 km/h. **(A)** T_j-T_c combination **(B)** T_j-Mj combination **(C)** T_j-Mc combination **(D)** T_c-Mj combination **(E)** T_c-Mc combination **(F)** Mj-Mc combination.

TABLE 5 The variation trend of standard deviation with parameters.

Parameter combination	Direction of Fstd reduction	Direction of Fstd increase
(T_j, T_c)	(1.2, 1.2)	(0.8, 0.8)
(T_j, Mj)	(1.2, 0.8)	(0.8, 1.2)
(T_j, Mc)	(1.2, 0.8)	(0.8, 1.2)
(T_c, Mj)	(1.2, 0.8)	(0.8, 1.2)
(T_c, Mc)	(1.2, 0.8)	(0.8, 1.2)
(Mj, Mc)	(0.8, 0.8)	(1.2, 1.2)

From the above analysis, it can be seen that the tension of the contact wire, the tension of the catenary wire, and the linear density of the contact wire have a consistent influence on the contact pressure under mutual combinations, while the influence of the linear density of the catenary wire is not very consistent. Therefore, this paper proposes the following optimization schemes. As shown in Table 7.

According to the optimized parameter settings in Table 7, the contact pressures obtained under several schemes are compared with the contact pressure before optimization, as shown in Figures 11, 12.

As can be seen from Figures 11, 12, when two parameters are optimized simultaneously, the peak value of contact pressure is greatly reduced. The maximum contact pressure is reduced to below 250 N. The average contact pressure increases, and the standard deviation value is significantly reduced. The offline rate is greatly reduced. When three parameters are changed simultaneously, the optimization effect on contact pressure is more obvious. The standard deviation of contact pressure is further reduced, and the offline rate is reduced to within 1%. It fully meets the requirements of pantograph-catenary current collection quality. In conclusion, at a running speed of 500 km/h, by increasing the contact wire tension, reducing the catenary wire tension, and reducing the contact wire density, a catenary structure can be optimized to make the pantograph-catenary operation result very ideal.

5 Conclusion

The pantograph-catenary coupling finite element model is established by using MSC. Marc software. The influence of single parameter change of catenary on contact pressure is analyzed. Then, the response surface method is introduced to study the influence of the combined change of two parameters on contact pressure. Finally, based on the influence of multiple parameters, the catenary structure parameters with a running speed of 500 km/h are optimized, and the following conclusions are obtained:

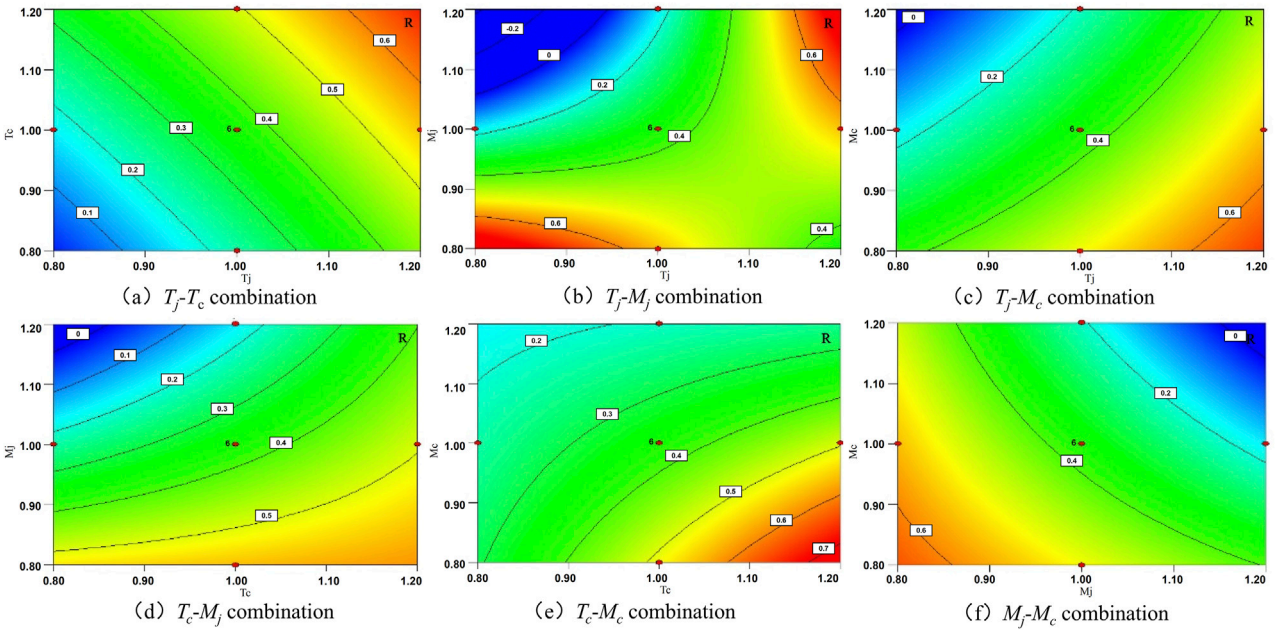

FIGURE 10
Contour map of off-line rate at 500 km/h. **(A)** T_j-T_c combination **(B)** T_j-Mj combination **(C)** T_j-Mc combination **(D)** T_c-Mj combination **(E)** T_c-Mc combination **(F)** Mj-Mc combination.

TABLE 6 Variation trend of off-line rate with parameters.

Parameter combination	Direction of *r* reduction	Direction of *r* increase
(T_j, T_c)	(0.8, 0.8)	(1.2, 1.2)
(T_j, Mj)	(1.2, 1.2)	(0.8, 0.8)
(T_j, Mc)	(0.8, 1.2)	(1.2, 0.8)
(T_c, Mj)	(0.8, 1.2)	(1.2, 0.8)
(T_c, Mc)	(0.8, 1.2)	(1.2, 0.8)
(Mj, Mc)	(1.2, 1.2)	(0.8, 0.8)

TABLE 7 Optimization design scheme of catenary parameters for high-speed projectile chain with a speed of 500 km per hour.

Serial Number	Changed parameter	Parameter optimization design
0	—	Tj = 27kNj, Tc = 21kNj, Mj = 1.08kg/mj, Mc = 1.08 kg/m
1	Tj	Tj = 32.4kNj, Tc = 21kNj, Mj = 1.08kg/mj, Mc = 1.08 kg/m
2	Tc	Tj = 27kNj, Tc = 25.2kNj, Mj = 1.08kg/mj, Mc = 1.08 kg/m
3	Mj	Tj = 27kNj, Tc = 21kNj, Mj = 0.864kg/mj, Mc = 1.08 kg/m
4	Tj, Tc	Tj = 32.4kNj, Tc = 25.2kNj, Mj = 1.08kg/mj, Mc = 1.08kg/
5	Tjj, Mj	Tj = 32.4kNj, Tc = 21kNj, Mj = 0. 864kg/mj, Mc = 1.08 kg/m
6	Tjj, Tcj, Mj	Tj = 32.4kNj, Tc = 25.2kNj, Mj = 0. 864kg/mj, Mc = 1.08 kg/m

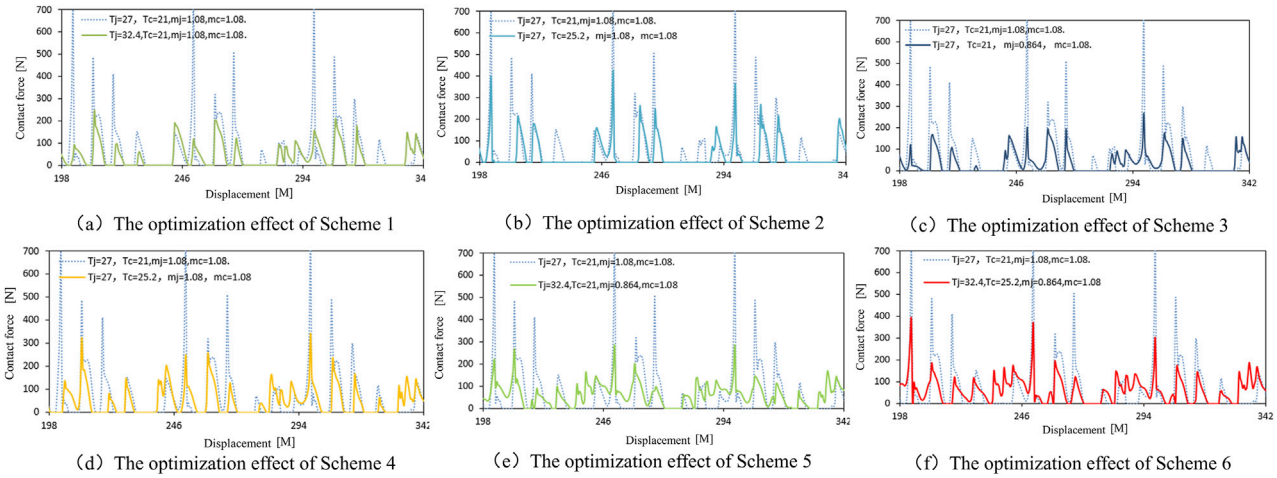

FIGURE 11
Comparison of contact pressure change curves before and after optimization. **(A)** The optimization effect of Scheme 1 **(B)** the optimization effect of Scheme 2 **(C)** the optimization effect of Scheme 3 **(D)** the optimization effect of Scheme 4 **(E)** the optimization effect of Scheme 5 **(F)** the optimization effect of Scheme 6.

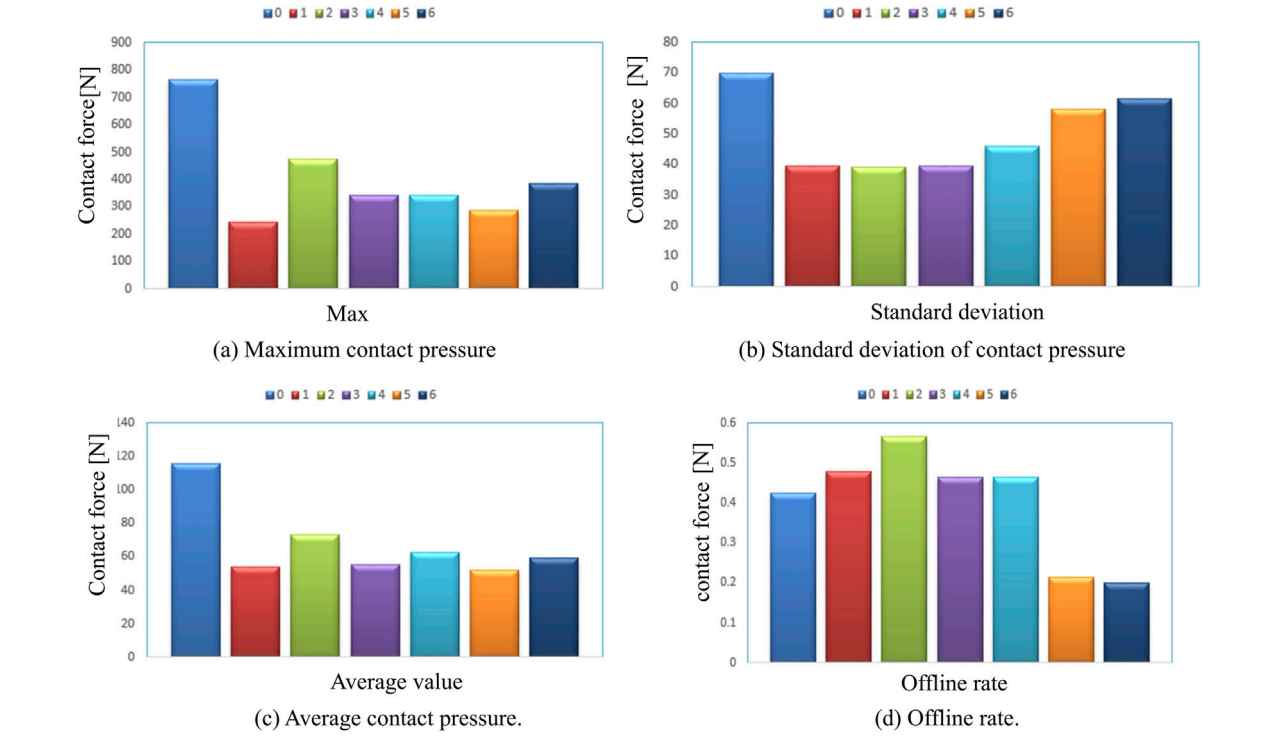

FIGURE 12
Comparison of statistical values of contact pressure before and after optimization. **(A)** Maximum contact pressure **(B)** standard deviation of contact pressure **(C)** average contact pressure **(D)** offline rate.

(1) When the catenary parameters change singly, within a certain range, increasing the contact wire tension, reducing the catenary wire tension, reducing the contact wire linear density, and reducing the catenary wire linear density can improve the pantograph-catenary current collection quality.
(2) Based on the response surface analysis method, when two parameters are combined with each other, the contact wire tension, catenary wire tension and contact wire linear density have basically the same influence on the average value and standard deviation of contact pressure. When the catenary wire linear density is combined with the wire tension respectively, the change of wire tension has a greater influence on contact pressure, and the influence of catenary wire linear density is smaller.
(3) In order to optimize the catenary at 500 km/h, under the conditions of increasing the contact wire tension, reducing the catenary wire tension and reducing the contact wire linear density, the average value of contact pressure is increased, the standard deviation, maximum value and offline rate of contact pressure are reduced, and the pantograph-catenary current collection quality is significantly improved.

Data availability statement

The original contributions presented in the study are included in the article/supplementary material, further inquiries can be directed to the corresponding author.

Author contributions

ZZ: Conceptualization, Data curation, Formal Analysis, Funding acquisition, Investigation, Methodology, Project administration, Resources, Software, Supervision, Validation, Visualization, Writing–original draft, Writing–review and editing. MZ: Investigation, Project administration, Resources, Visualization, Writing–original draft, Writing–review and editing.

Funding

The author(s) declare that financial support was received for the research, authorship, and/or publication of this article. ZZ would like to acknowledge financial support from the Special Scientific Research Program of the Education Department of Shaanxi Province (Project No. 24JK0615).

Conflict of interest

Author MZ was employed by China Construction Third Engineering Bureau Co., Ltd.

Generative AI statement

The author(s) declare that no Generative AI was used in the creation of this manuscript.

Publisher's note

References

Aboshi, M., and Manabe, K. (2000). Analyses of contact force fluctuation between catenary and pantograph. *Q. Rep. RTRI* 41 (4), 182–187. doi:10.2219/rtriqr.41.182

Bartz-Beielstein, T., Chiarandini, M., Paquete, L., and Preuss, M. (2010). *Experimental methods for the analysis of optimization algorithms* (Berlin: Springer).

Bruni, S., Bucca, G., Carnevale, M., Collina, A., and Facchinetti, A. (2018). Pantograph–catenary interaction: recent achievements and future research challenges. *Int. J. Rail Transp.* 6 (2), 57–82. doi:10.1080/23248378.2017.1400156

Cho, Y. H., Lee, K., Park, Y., Kang, B., and Kim, K.-nam (2010). Influence of contact wire pre-sag on the dynamics of pantograph–railway catenary. *Int. J. Mech. Sci.* 52 (11), 1471–1490. doi:10.1016/j.ijmecsci.2010.04.002

EN50318 (2002). "Railway applications-Current collection system-Validation of simulation of the dynamic interaction between pantograph and overhead contact line."

Jin, H. L., Park, T. W., Oh, H. K., and Kim, Y. G. (2015). Analysis of dynamic interaction between catenary and pantograph with experimental verification and performance evaluation in new high-speed line. *Veh. Syst. Dyn.* 53 (8), 1117–1134. doi:10.1080/00423114.2015.1025797

Li, T., Qin, D., Zhou, N., Zhang, J., and Zhang, W. (2022). Numerical study on the aerodynamic and acoustic scale effects for high-speed train body and pantograph. *Appl. Acoust.* 196, 108886. doi:10.1016/j.apacoust.2022.108886

Liu, Y., Song, Y., Duan, F., and Liu, Z. (2024). Suppression of railway catenary galloping based on structural parameters' optimization. *Sensors* 24 (3), 976. doi:10.3390/s24030976

Liu, Z., Wang, H., Chen, H., Wang, X., Song, Y., and Han, Z. (2023b). Active pantograph in high-speed railway: review, challenges, and applications. *Control Eng. Pract.* 141, 105692. doi:10.1016/j.conengprac.2023.105692

Liu, Z., Yang, S., Gao, S., and Wang, H. (2023a). Review of perspectives on pantograph-catenary interaction research for high-speed railways operating at 400 km/h and above. *IEEE Trans. Transp. Electrification* 10 (3), 7236–7257. doi:10.1109/TTE.2023.3346379

Lundstedt, T., Seifert, E., Abramo, L., Thelin, B., Nyström, Å., Pettersen, J., et al. (1998). Experimental design and optimization. *Chemom. intelligent laboratory Syst.* 42 (1-2), 3–40. doi:10.1016/s0169-7439(98)00065-3

Luo, Q., Mei, G., Chen, G., and Zhang, W. (2024). Study of pantograph-catenary system dynamic in crosswind environments. *Veh. Syst. Dyn.* 62 (4), 813–836. doi:10.1080/00423114.2023.2199456

Massat, J. P., Laine, J. P., and Bobillot, A. (2006). Pantograph–catenary dynamics simulation. *Veh. Syst. Dyn.* 44 (Suppl. 1), 551–559. doi:10.1080/00423110600875443

Park, T.-J., Han, C.-S., and Jang, J.-H. (2003). Dynamic sensitivity analysis for the pantograph of a high-speed rail vehicle. *J. Sound Vib.* 266 (2), 235–260. doi:10.1016/s0022-460x(02)01280-4

Pombo, J., and Ambrósio, J. (2012). Influence of pantograph suspension characteristics on the contact quality with the catenary for high speed trains. *Comput. and Struct.* 110, 32–42. doi:10.1016/j.compstruc.2012.06.005

Pombo, J., Ambrósio, J., Pereira, M., Rauter, F., Collina, A., and Facchinetti, A. (2009). Influence of the aerodynamic forces on the pantograph–catenary system for high-speed trains. *Veh. Syst. Dyn.* 47 (11), 1327–1347. doi:10.1080/00423110802613402

Song, Y., Lu, X., Yin, Y., Liu, Y., and Liu, Z. (2024). Optimization of railway pantograph-catenary systems for over 350 km/h based on an experimentally validated model. *IEEE Trans. Industrial Inf.* 20, 7654–7664. doi:10.1109/tii.2024.3361485

Su, K., Zhang, J., Zhang, J., Yan, T., and Mei, G. (2023). Optimisation of current collection quality of high-speed pantograph-catenary system using the combination of artificial neural network and genetic algorithm. *Veh. Syst. Dyn.* 61 (1), 260–285. doi:10.1080/00423114.2022.2045029

Wang, X., Liu, Z., Song, Y., Hu, G., Zhou, S., Duan, F., et al. (2024). Structural performance analysis and optimization design of railway pantograph under high-speed operating conditions. *IEEE Trans. Instrum. Meas.* 73, 1–14. doi:10.1109/tim.2024.3470994

Wu, G., Dong, K., Xu, Z., Xiao, S., Wei, W., Chen, H., et al. (2022). Pantograph–catenary electrical contact system of high-speed railways: recent progress, challenges, and outlooks. *Railw. Eng. Sci.* 30 (4), 437–467. doi:10.1007/s40534-022-00281-2

Zhang, W., Liu, Yi, and Mei, G. (2006). Evaluation of the coupled dynamical response of a pantograph—catenary system: contact force and stresses. *Veh. Syst. Dyn.* 44 (8), 645–658. doi:10.1080/00423110600744656

Zhou, N., and Zhang, W. (2011). Investigation on dynamic performance and parameter optimization design of pantograph and catenary system. *Finite Elem. analysis Des.* 47 (3), 288–295. doi:10.1016/j.finel.2010.10.008

Zhou, N., Zhang, W.-hua, and Li, R.-ping (2011). Dynamic performance of a pantograph-catenary system with the consideration of the appearance characteristics of contact surfaces. *J. Zhejiang University-SCIENCE A* 12 (12), 913–920. doi:10.1631/jzus.a11gt015